CORA Cork Open Research Archive
Cartlann Taighde Oscailte Chorcaí

Title	Structural and electrical Investigation of MoS2 thin films formed by thermal assisted conversion of Mo metal
Author(s)	Duffy, Ray; Foley, Patrick; Filippone, Bruno; Mirabelli, Gioele; O'Connell, Dan; Sheehan, Brendan; Carolan, Pat; Schmidt, Michael; Cherkaoui, Karim; Gatensby, Riley; Hallam, Toby; Duesberg, Georg; Crupi, Felice; Nagle, Roger; Hurley, Paul K.
Publication date	2016-06-30
Original citation	Duffy, R., Foley, P., Filippone, B., Mirabelli, G., O'Connell, D., Sheehan, B., Carolan, P., Schmidt, M., Cherkaoui, K., Gatensby, R., Hallam, T., Duesberg, G., Crupi, F., Nagle, R. and Hurley, P. K. (2016) 'Structural and Electrical Investigation of MoS2 Thin Films Formed by Thermal Assisted Conversion of Mo Metal', ECS Journal of Solid State Science and Technology, 5(11), pp. Q3016-Q3020.
Type of publication	Article (peer-reviewed)
Link to publisher's version	http://dx.doi.org/10.1149/2.0041611jss Access to the full text of the published version may require a subscription.
Rights	**© 2016 IEEE. Personal use of this material is permitted. Permission from IEEE must be obtained for all other uses, in any current or future media, including reprinting/republishing this material for advertising or promotional purposes, creating new collective works, for resale or redistribution to servers or lists, or reuse of any copyrighted component of this work in other works.**
Item downloaded from	http://hdl.handle.net/10468/3489

Downloaded on 2017-02-12T06:30:42Z

UCC
University College Cork, Ireland
Coláiste na hOllscoile Corcaigh

Structural and electrical investigation of MoS_2 thin films formed by thermal assisted conversion of Mo metal

Ray Duffy,[1] Patrick Foley,[1] Bruno Filippone,[1,2] Gioele Mirabelli,[1,2] Dan O'Connell,[1] Brendan Sheehan,[1] Pat Carolan,[1] Michael Schmidt,[1] Karim Cherkaoui,[1] Riley Gatensby,[3,4] Toby Hallam,[3,4] Georg Duesberg,[3,4] Felice Crupi,[2] Roger Nagle,[1] Paul K. Hurley.[1]

[1] Tyndall National Institute, University College Cork, Cork, Ireland.

[2] University of Calabria, Arcavacata di Rende, Italy.

[3] Centre for Research on Adaptive Nanostructures and Nanodevices (CRANN), Trinity College Dublin, Dublin 2, Ireland.

[4] School of Chemistry, Trinity College Dublin, Dublin 2, Ireland.

ABSTRACT

Large-area synthesis is of great demand for the preparation of high-performance transition-metal-dichalcogenides (TMD) devices, however there are only limited reports to date of device operation on large-area TMDs. In this work we fabricate MoS_2 devices based on Thermal Assisted Conversion (TAC) of metal layers, and characterise the thin-films with material analysis combined with electrical device parameter extraction. Specifically we report on temperature dependent parameter extraction for Ti/Au contacts to MoS_2 thin-films to determine sheet resistance (R_{sh}), resistivity (ρ), and the activation energy (E_A) of on-state current flow. For undoped MoS_2, ρ was determined to be 191 Ω.cm at 25 °C. The activation energy of the on-state current was found to be 0.18 eV, pointing to the presence of deep levels in MoS_2.

INTRODUCTION

Due to the performance and economic benefit obtained by scaling, future semiconductor electron devices for logic functions will progress toward ultra-thin-body channels and 2-dimensional (2D) high carrier mobility materials. The significance is that small devices can be made to yield higher performance and greater energy-efficiency. To put this trend in perspective, fin-field-effect-transistor[1,2] (FinFET) technology was a research topic 7-8 years ago, but is now at the heart of the microprocessor in high-end smartphones.[3] While the positioning of TMDs in electronic products of the future is still unsure, perhaps they will be more suited to low power, it is still worthwhile to understand how a relatively undeveloped system can reach maturity in less than a decade.

Graphene is semi-metallic, which makes it difficult to switch off electron devices such as FETs. Bandgap engineering is required to open a bandgap of graphene, which is not an easy undertaking. This has motivated the scientific community to search for alternate 2D layer materials with semiconducting properties and better tuneability. Many TMDs are natural semiconductors with thicknesses on the nanometre scale. TMD semiconductors are now emerging as potentially useful materials, where more research is needed, in order to explore their properties and potential applications.

The properties of a single- and few-layer TMDs are very distinct from those of the bulk, such as a transition from indirect to direct semiconductor.[4,5,6,7] Furthermore, as a result of both the reduced dimension and modified electronic structure these materials have great potential for applications in electronics, energy storage and conversion,[8] as well as sensors.[9] TMD materials are comprised of single-atomic layers of transition metal atoms (e.g. Mo) sandwiched between layers of group-VI atoms (e.g. S). These repeated units are held together via van der Waals bonding. This combination of strong covalent intra-plane and weak inter-plane bonding allows for 2D synthesis of TMDs.

Due to being surface-dominated, the properties of TMDs vary considerably with the number of layers in a sheet, and surface termination can dramatically alter the material properties. In terms of optimum TMD thickness, Das et al. did a systematic study on MoS_2 flakes, fabricating back-gated n-type FET devices.[10] Based on drive current and mobility, MoS_2 thicknesses of ~6-12 nm appears to be optimum. Radisavljevic et al. reported top-gated MoS_2 FETs, based on monolayer flakes with an Atomic Layer Deposition (ALD) 30 nm HfO_2 gate dielectric, which produced a 10^8 on-off current ratio at a gate length of 3 μm.[11] Using a dual-gate device architecture Liu et al. made MoS_2 n-type FETs on flakes, and produced an over 10^8 on-off current ratio.[12] Note these were long channel devices with drive current outputs much lower than that of the state-of-the-art Si equivalent. It was concluded by the authors that device performance at small gate lengths is limited by contact resistance,[13] making it a key bottleneck for realisation of these devices in future technologies.

The ITRS Roadmap[14] has cited the Difficult Challenge in the 2018-2026 timeframe "Develop 2nd generation new materials to replace silicon (or InGaAs, Ge) as an alternate channel and source/drain to increase the saturation velocity and to further reduce V_{DD} and power dissipation in MOSFETs". To date, MoS_2 has been the testing ground for many TMD based experiments due to its relative stability in ambient conditions.

As the fabrication of high quality substrates is usually the starting point of any semiconductor activity, the reliable synthesis of 2D materials is an essential first step. Many experimental studies to date feature mechanical exfoliation[15,16,17] of large crystals or "flakes", or chemical solution-based exfoliation by dispersion in a solvent.[18,19] Indeed many TMD device reports in the literature are based on flakes of material.[20,21,22,23,24,25,26,27,28]

While this is an effective starting point, say in the screening process of candidate materials, this method is not compatible with production or manufacturing environment. Large-area synthesis is of great demand for the preparation of high-performance devices. To

that end, vapour deposition stands as an appealing and versatile approach to form synthetic TMD thin films. Recently MoS_2 layers have been fabricated using Chemical Vapour Deposition (CVD) techniques.[29,30] H. Liu et al. synthesised MoS_2 top-gated n-type FET devices using CVD,[31] and performed electrical analysis of ~100 devices. Gatensby et al. presented a route to the manufacture of devices from MoS_2 and WS_2, grown by thermally assisted conversion (TAC) of pre-deposited metal layers, producing sensors with a sensitivity to NH_3 down to 400 ppb.[32] Recently X. Liu et al. fabricated monolayer MoS_2 by CVD under atmospheric pressure and characterised the peak field effect mobility in FET devices at 59 $cm^2V^{-1}s^{-1}$.[33]

To date experiments probing the electronic properties of these 2D materials remain at an early stage of development, particularly on large area films grown by TAC or ALD. In this work we perform parameter extraction for MoS_2 thin-films formed by TAC of Mo in a sulphur vapour to determine sheet resistance (R_{sh}), resistivity (ρ), and activation energy (E_A) of the on-state current flow.

EXPERIMENTAL

MoS_2 films were formed on 300 nm SiO_2 on p^+ Si handle wafers. The sample sizes were approximately 1×1 cm^2. Mo was deposited by evaporation, nominal thicknesses were in the range of 5-30 nm. Substrates were placed in a quartz tube furnace and heated (~50 °C /min) to 500 °C under Ar flow (150 sccm, P ~0.7 Torr). After a 5 min dwell at 500 °C, the samples were heated to 750 °C (25 °C /min) and annealed for 15 min. A second upstream hot zone was used to heat the S powder to 113 ± 1 °C, and thus introduce S vapour into the reaction zone. This hot zone consisted of an assembly of halogen bulbs coupled with a power supply. A k-type thermocouple, placed alongside the S supply, allowed for the temperature in the vicinity of the S powder to be monitored. Following TAC, the samples were held at 750

°C for a further 30 min, before the furnace was cooled. Upon removal from the furnace, samples were cleaned with acetone and then isopropanol to remove unreacted residue. Finally, samples were subsequently stored in N_2 and shipped in vacuum packaging.

Thereafter MoS_2 circular Transfer Length Method (C-TLM) structures were fabricated using a metal lift-off process. After resist processing and patterning, 10 nm of Ti and 90 of Au were deposited as contacts. The use of the lift-off process and a circular geometry for the TLM structures allowed the definition of devices without the requirement to etch the MoS_2 film.

For analysis, cross-section samples were obtained by using FEI's Dual Beam Quanta 3D 200i. On top of the MoS_2 three layers of protective material were used, namely electron beam TEOS, electron beam W, and ion beam Pt. Lamellas were thinned and polished at 30 kV 100 pA and 5 kV 48 pA respectively on FEI Dual Beam Helios Nanolab 600i system using a Ga ion beam. Transmission Electron Microscopy (XTEM) imaging was carried out using a JEOL 2100 HRTEM operated at 200 kV in Bright Field mode using a Gatan Double Tilt holder. Electrical measurements were performed on-wafer in a microchamber probe station (Cascade, Summit 12971B) in a dry air, dark environment (dew point ≤203K).

RESULTS AND DISCUSSION

Fig 1(a) shows a wide view of MoS_2 on a SiO_2/Si substrate for a sample with an initial Mo thickness of 10 nm. On the right-hand side the Ti/Au metal contact is visible. The MoS_2 layer is continuous across the surface and the deposition and patterning of the metal contact has not made an obvious impact on the MoS_2. The layered structure of MoS_2 is visible in the higher resolution image in Fig. 1(b). The MoS_2 is not perfectly layered but is poly-crystalline in nature. From XTEM the MoS_2 thickness was estimated to be 20 nm.

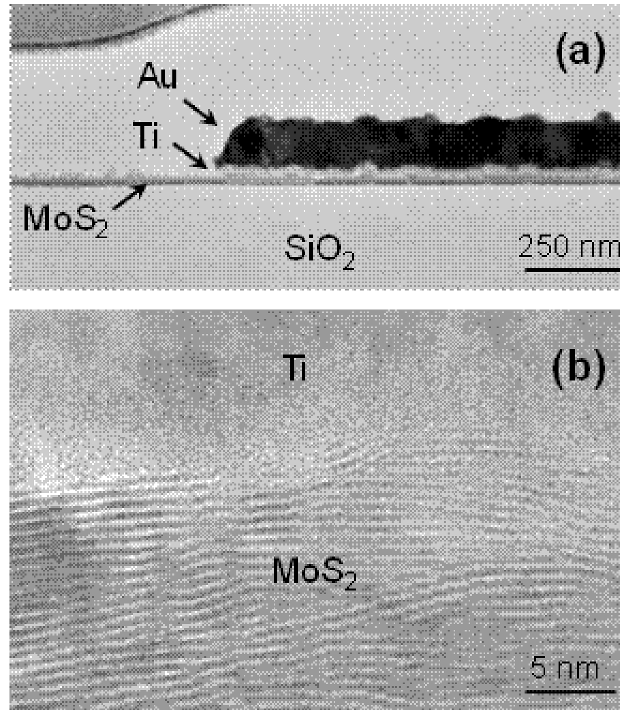

Fig. 1 : Representative images of the 10 nm Mo after TAC, forming approximately 20 nm of MoS_2. (a) A wide view of MoS_2 on a SiO_2/Si substrate. On the right-hand side the Ti/Au metal contact is visible. The MoS_2 layer is continuous across the surface. (b) The layered structure of MoS_2 is visible in the higher resolution image.

For a TAC process it is important to sulphurise the entire Mo layer, otherwise it's possible the MoS_2 will lie on top of unreacted Mo, which would as act as a short circuit in an electron device. A check for this can be done by extracting the lattice d-spacing via the XTEM images. Lattice resolution images were first obtained to determine the d-spacings. Measured values were compared with database values [34] to identify whether the layers were Mo or MoS_2. We performed Fast-Fourier-Transform (FFT) analysis of the XTEM image shown in Fig. 2(a) for a situation where some Mo was left unreacted. In that case the initial Mo thickness was 30 nm. The lattice d-spacings can be extracted from the FFT, and based on this the material can be identified. The lattice d-spacing was determined to be 2.3 Angstroms in the dark spots below the MoS_2 which corresponds to the lattice spacing in Mo. The d-spacing of 6.1 Angstroms confirms the layer marked "MoS_2" is indeed MoS_2. For

comparison the sample with an initial 10 nm Mo layer is shown in Fig. 2(b) post-TAC. Fig. 2(c) schematically shows the lattice spacing in MoS_2.

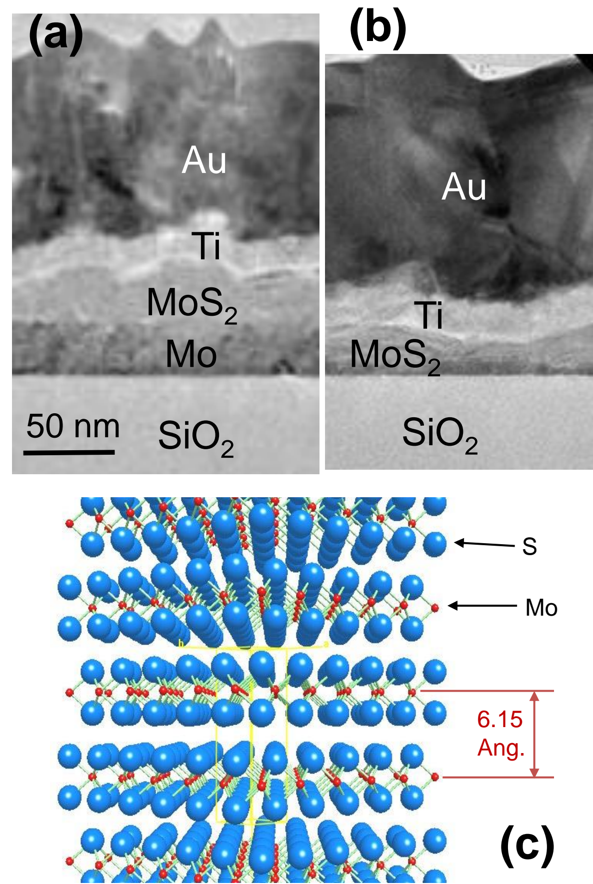

Fig. 2 : (a) Representative image of 30 nm Mo after TAC, forming MoS_2 laying on top of unreacted Mo. (b) Representative image of 10 nm Mo after TAC, completely converted to MoS_2. (c) A schematic shows the lattice spacing in MoS_2. The lattice spacing of 6.15 Angstrom allows us to identify the regions of MoS_2.

The electrical data presented hereafter is for the completely-converted Mo film, as in Figs. 1 and 2(b). Fig. 3 shows the electrical current-voltage behaviour extracted from the C-TLM structure. An optical image of the structure is shown in the inset. The individual curves represent different contact spacings. The current is ohmic in nature, it is linear with respect to voltage and goes through the origin. The current scales with contact spacing, as expected. For samples where the Mo is not totally converted, the current-voltage characteristics were non-linear, with no clear dependence on contact separation (not shown).

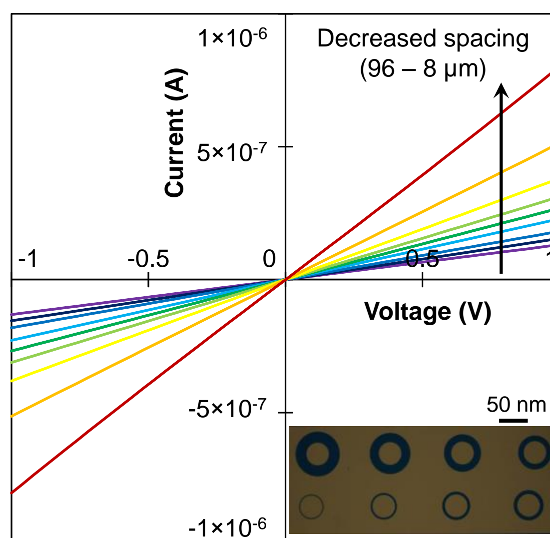

Fig. 3 : Representative measured current versus voltage characteristic in the MoS_2 circular TLM structure as a function of contact spacing. The Mo thickness was 10 nm prior to TAC. The current is linear with respect to voltage and passes through the origin. The current increases with decreased contact spacing as expected. The inset shows an optical image of the circular TLM structure.

The temperature dependence of the current was then evaluated. Representative data is shown in Fig. 4 for a contact spacing of 80 μm. The current versus voltage behaviour is still linear up to 100 °C, and the current increases with increasing temperature consistent with semiconductor behaviour. Fig. 5 shows I versus 1/kT which is used to extract the activation energy (E_A) of the on-state current, which was found to be 0.18 eV. The bandgap of MoS_2 in bulk form is 1.3 eV, increasing to 1.8 eV in monolayer form,[10] as the nature of the band gap changes from indirect to direct.[35] The value of activation energy obtained here agrees with the value determined by Kam-Keung, where a value of 0.1 eV activation energy of electrical resistivity was reported in 1982.[36] An activation energy in this range is consistent with an unintentional deep dopant level in the MoS_2. Recently Cavalho et al. reported Density Functional Theory calculations of various impurities in MoS_2, such as substitutional halogens, where Cl and Br are found to introduce deep donor levels at 0.18 eV and 0.15 eV below the conduction band edge respectively.[37]

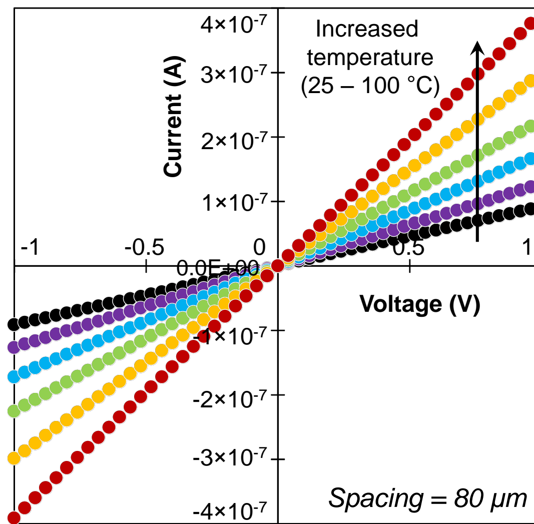

Fig. 4 : Measured current versus voltage characteristic in the MoS_2 circular TLM structure for different temperatures. The Mo thickness was 10 nm prior to TAC. The temperature dependence is consistent with a semiconductor behaviour.

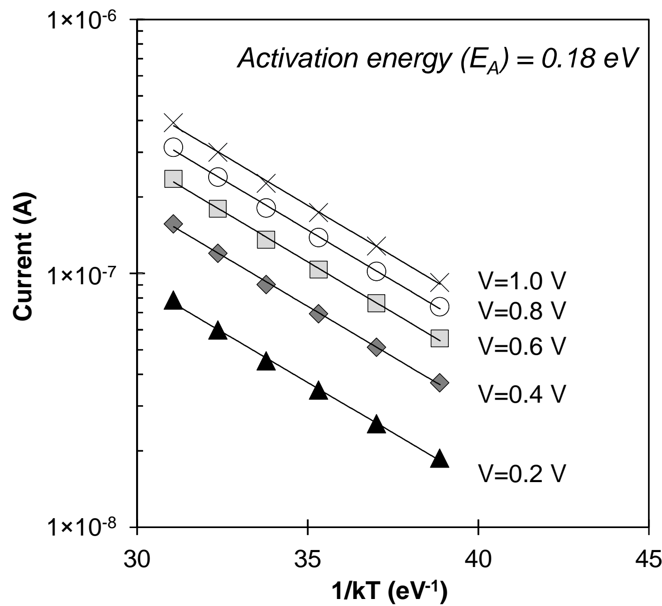

Fig. 5 : Measured current versus 1/kT (symbols) and Arrhenius fits (lines) for different voltages. At each voltage E_A was determined to be 0.18 eV.

Total resistance (R_T) was then calculated and plotted versus contact spacing. In accordance with C-TLM theory, R_T must be corrected to account for the circular nature of the structures, before a linear fit is made. This linearisation of R_T is performed according to the equations :

$$R_T = \frac{R_{sh}}{2\pi L}(d + 2L_T)C \quad (1)$$

$$C = \frac{L}{d} ln\left(1 + \frac{d}{L}\right) \quad (2)$$

where R_{sh} is sheet resistance, L_T is the transfer length, L is the inner contact radius in the C-TLM test structure, and d is the contact separation. C is a correction factor to account for the circular nature of the test structure. Once applied, we obtain the corrected total resistance;

$$R_{T_COR} = \frac{R_{sh}}{2\pi L}(d + 2L_T) \quad (3)$$

The linear interpolation of R_{T_COR} versus d (see Fig. 6) allows us to estimate R_{sh} and L_T. From the knowledge of these parameters, we can evaluate the resistivity (ρ) and the specific contact resistivity (ρ_c) as follows:

$$\rho = R_{sh}.t \quad (4)$$

$$\rho_c = R_{sh}.{L_T}^2 \quad (5)$$

where t is the MoS_2 thickness.

The dependence of the total resistance as a function of contact separation over the temperature range (25 °C to 100 °C) is shown in Figure 6. Note, both slope and intercept of this linear fit line changes with temperature, indicating a change in both contact resistance and bulk MoS_2 resistivity with temperature. R_{sh} was estimated to be 95.8 MΩ/sq at 25 °C, dropping down to 20.3 MΩ/sq at 100 °C. Taking into account the MoS_2 thickness of 20 nm in Eqn. (4) ρ decreases from 191 Ω.cm at 25 °C to 41 Ω.cm at 100 °C (see Fig. 7). The 25 °C value of bulk resistivity is around one order of magnitude higher than the resistivity reported for natural crystal of MoS_2 by Grant et al, which was found to be 18 Ω.cm with a 6×10^{15} cm^{-3} n-type doping level.[38] The values of transfer length obtained from the intercept of the y-axis are around 2.57 to 2.34 µm at 25 and 100 °C, yielding values of specific contact resistivity for the Au/Ti/MoS_2 contacts of 6.3 to 1.1 $\Omega.cm^2$ respectively. These values of specific contact

resistivity are clearly too high for device applications, but this thin-film is not intentionally doped, and no attempt has been made in this work to reduce this value. Sheet resistance and specific contact resistivity can be modified by doping techniques. For example, Du et al. reported molecular doping of 4-5 nm thick MoS_2 by polyethyleneimine.[39] After doping the MoS_2 R_{sh} was approximately 20 kΩ/sq, so according to Eqn. (4) ρ was reduced to approximately 10^{-2} Ω.cm. Chloride molecular doping also appears to hold promise.[40] Rai et al. used amorphous titanium suboxide encapsulation to reduce monolayer MoS_2 R_{sh} to 12.4 kΩ/sq, which is an impressive ρ value of <10^{-3} Ω.cm.[41]

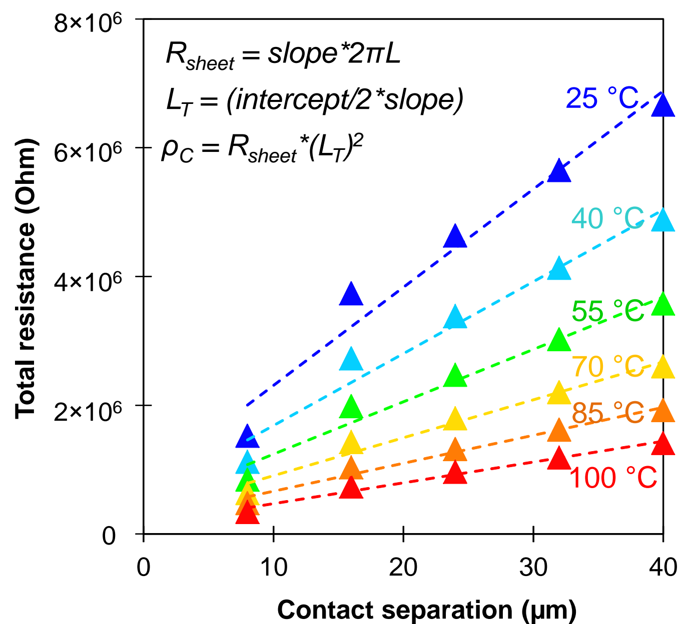

Fig. 6 : Linearised total resistance versus contact spacing as a function of temperature, which is used to extract sheet resistance and MoS_2 resistivity. The Mo thickness was 10 nm prior to TAC.

It can also be considered whether changes with temperature in bulk or sheet resistivity could be decoupled from changes in the contact resistance. We see in Fig. 6 that both the slope and intercepts of the linear fit lines change, not just one changing with the other fixed. In other words we found that all resistivity parameters (R_{sh}, ρ_c) fall by approximately the same level, 80 %, in going from 25 to 100 °C.

Finally, there have been a number reports in literature of MoS_2 flake device performance in vacuum. W. Liu et al. presented improved device performance when TMD FETs were measured after 380 K 1 hr anneal to remove absorbed molecules at the surface, and measured under vacuum conditions.[42] The electrical characteristics here were re-measured over a period of weeks. Shown in Fig. 7 are MoS_2 bulk resistivity values before and after air exposure for 1 month. At 25 °C there is a 13 % increase due to 1 month air exposure. It is noted that the MoS_2 samples studied in this work were not passivated and the MoS_2 surface is exposed to air in the regions outside the Au/Ti contacts. For sensor applications one would have to consider reversibility, if the MoS_2 converts to molybdenum-oxide of some form then this might not be easily reversible. For electronic applications care must be taken to properly encapsulate the MoS_2.

It should be noted that this air sensitivity is not specific to TMDs formed by TAC. We have seen significant air sensitivity of mechanically exfoliated TMDs of various types. That work will be presented elsewhere.

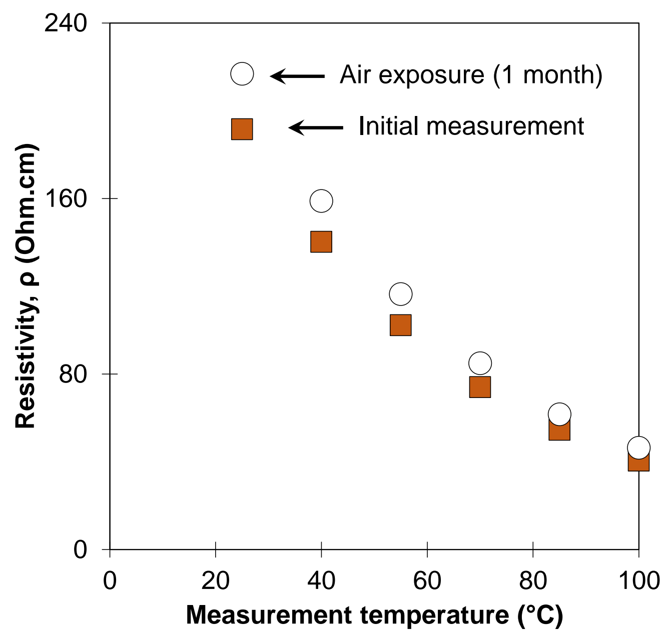

Fig. 7 : Resistivity (ρ) changes with air exposure. Orange points correspond to the initial measurements while the white points correspond to after 1 month of air exposure. At 25 °C there is a 13 % increase due to 1 month air exposure.

CONCLUSIONS

In this work we structurally and electrically characterised large-area synthesised MoS_2 devices, formed by a thermally assisted conversion process. The bulk resistivity of the nominally undoped MoS_2 was determined to be 191 Ω.cm at 25 °C, extracted from circular Transfer Length Method structures with Ti/Au contacts. The activation energy of the conduction current over the temperature range 25-100 °C was determined to be 0.18 eV, consistent with the presence of deep donor levels in the MoS_2. The transfer length was around 2.57 to 2.34 μm at 25 and 100 °C, yielding values of specific contact resistivity for the Au/Ti/MoS_2 contacts of 6.3 to 1.1 Ω.cm^2 respectively. This high resistivity values indicate the requirement for local source and drain doping of the MoS_2 practical device applications. When exposed to air for 1 month the MoS_2 resistivity was observed to increase by 13%, thus for certain applications care must be taken to properly passivate or encapsulate the TMD layers.

ACKNOWLEDGEMENTS

This work is supported by the Science Foundation Ireland under Contract No. 12/RC/2278 and PI_10/IN.1/I3030. We also acknowledge the support of Science Foundation Ireland through the US-Ireland R&D Partnership Programme "*Understanding the Nature of Interfaces in Two Dimensional Electronics (UNITE)*" Grant Number SFI/13/US/I2862. The research was supported in part by the Higher Education Authority Programme for Research in Third Level Institutions in Ireland under Grant Agreement no. HEA PRTLI5.

REFERENCES

[1] J. –P. Colinge (Ed.), "*FinFETs and other Multi-Gate Transistors*" ISBN 978-0-387-71752-4, Springer (2008).
[2] N. Collaert (Ed.), "*CMOS Nanoelectronics: Innovative Devices, Architectures, and Applications*" ISBN 9789814364027, Pan Stanford (2012).
[3] J. Borland, ECS Transactions, 69 (10) 11-20 (2015).
[4] S. Z. Butler, S. M. Hollen, L. Cao, Y. Cui, J. A. Gupta, H. R. Gutierrez, T. F. Heinz, S. S. Hong, J. Huang, A. F. Ismach, E. Johnson-Halperin, M. Kuno, V. V. Plashnitsa, R. D. Robinson, R. S. Rouff, S. Salahuddin, J. Shan, L. Shi, M. G. Spencer, M. Terrones, W. Windl, and J. G. Goldberger, ACS Nano. **7**, 2898 (2013).
[5] X. Song, J. Hu, and H. Zeng, J. Mat. Chem. C. **1**, 2952 (2013).
[6] M. C. Lemme, L.-J. Li, T. Palacios, and F. Schwierz, MRS Bulletin **39**, 771 (2014).
[7] D. Jariwala, V. K. Sangwan, L. J. Lauhon, T. J. Marks, and M. C. Hersam, ACS Nano **8**, 1102 (2014).
[8] H. Nolan, N. McEvoy, M. O'Brien, N. C. Berner, C. Yim, T. Hallam, A. R. McDonald, G. S. Duesberg, Nanoscale **6**, 8185 (2014).
[9] K. Lee, R. Gatensby, N. McEvoy, T. Hallam, G. S. Duesberg, Advanced Materials **25**, 6699 (2013).
[10] S. Das, H. –Y. Chen, A. V. Penumatcha, and J. Appenzeller, Nano. Lett. 13, 100 (2013).
[11] B. Radisavljevic, A. Radenovic, J. Brivio, V. Giacometti, and A. Kis, Nature Nano. **6**, 147 (2011).
[12] H. Liu and P. D. Ye, IEEE El. Dev. Lett. **33**, 546 (2012).
[13] H. Liu, A. T. Neal, and P. D. Ye, ACS Nano. **6**, 8563 (2012).
[14] www.itrs.net
[15] J. N. Coleman, M. Lotya, A. O'Neill, S. D. Bergin, P. J. King, U. Khan, K. Young, A. Gaucher, S. De, R. J. Smith, I. V. Shvets, S. K. Arora, G. Stanton, H. Y. Kim, K. Lee, G. T. Kim, G. S. Duesberg, T. Hallam, J. J. Boland, J. J. Wang, J. F. Donegan, J. C. Grunlan, G. Moriarty, A. Shmeliov, R. J. Nicholls, J. M. Perkins, E. M. Grieveson, K. Theuwissen, D. W. McComb, P. D. Nellist, V. Nicolosi, Science **331**, 568 (2011).
[16] F. K. Perkins, A. L. Friedman, E. Cobas, P. M. Campbell, G. G. Jernigan, B. T. Jonker, Nano Lett. **13**, 668 (2013).
[17] D. J. Late, Y. -K. Huang, B. Liu, J. Acharya, S. N. Shirodkar, J. Luo, A. Yan, D. Charles, U. V. Waghmare, V. P. Dravid, C. N. R. Rao, ACS Nano **7**, 4879–4891 (2013).
[18] Q. He, Z. Zeng, Z. Yin, H. Li, S. Wu, X. Huang, H. Zhang, Small **8**, 2994–2999 (2012).
[19] Y. Yao, Z. Lin, Z. Li, X. Song, K.-S. Moon, C.-P. Wong, J. Mater. Chem. **22** 13494 (2012).
[20] K. Lee, H. Y. Kim, M. Lotya, J. N. Coleman, G. T. Kim, G. S. Duesberg, Advanced Materials **23**, 4178 (2011).
[21] M. Chen, H. Nam, S. Wi, L. Ji, X. Ren, L. Bian, S. Lu, and X. Liang, Appl. Phys. Lett. **103**, 142110 (2013).
[22] H. Fang, M. Tosun, G. Seol, T. C. Chang, K. Takei, J. Guo, and A. Javey, Nano. Lett. **13**, 1991 (2013).
[23] H. Fang, S. Chuang, T. C. Chang, K. Takei, T. Takahashi, and A. Javey, Nano. Lett. **13**, 3788 (2012).
[24] H. Liu, A. T. Neal, and P. D. Ye, ACS Nano. **6**, 8563 (2012).
[25] J. –R. Chen, P. M. Odenthal, A. G. Swartz, G. C. Floyd, H. Wen, K. Y. Luo, and R. K. Kawakami, Nano. Lett. **13**, 3106 (2013).

[26] W. S. Hwang, M. Remskar, R. Yan, T. Kosel, J. K. Park, B. J. Cho, W. Haensch, H. Xing, A. Saebaugh, and D. Jenai, Appl. Phys. Lett. **102**, 043116 (2013).
[27] J. Lin, J. Zhong, S. Zhong, H. Li, H. Zhang, and W. Chen, Appl. Phys. Lett. **103**, 063109 (2013).
[28] G. Mirabelli, M. Schmidt, B. Sheehan, K. Cherkaoui, S. Monaghan, I. Povey, M. McCarthy, A. P. Bell, R. Nagle, F. Crupi, P. K. Hurley, and R. Duffy, AIP Advances **6**, 025323 (2016).
[29] M. O'Brien, N. McEvoy, T. Hallam, H. –Y. Kim, N. C. Berner, D. Hanlon, K. Lee, J. N. Coleman, G. S. Duesberg, Scientific Reports **4**, 7374 (2015).
[30] S. Najmaei, Z. Liu, W. Zhou, X. Zou, G. Shi, S. Lei, B. I. Yakobson, J. –C. Idrobo, P. M. Ajayan, J. Lou, Nature Materials **12**, 754 (2013).
[31] H. Liu et al., Nano. Lett. **13**, 2640 (2013).
[32] R. Gatensby, N. McEvoy, K. Lee, T. Hallam, N. C. Berner, E. Rezvani, S. Winters, M. O'Brien, G. S. Duesberg, Appl. Surf. Sci. **297**, 139 (2014).
[33] X. Liu, J. He, Q. Liu, D. Tang, J. Wen, W. Liu, W. Yu, J. Wu, Z. He, Y. Lu, D. Zhu, W. Liu, P. Cao, S. Han, and K.-W. Ang, J. Appl. Phys. **118**, 124506 (2015).
[34] ICDD-PDF 88-2331
[35] K. F. Mak, C. Lee, J. Hone, J. Shan, and T. F. Heinz, Phys. Rev. Lett. 105, 136805 (2010).
[36] Kam-Keung Kam PhD thesis "*Electrical properties of WSe_2, WS_2, $MoSe_2$, MoS_2, and their use as photoanodes in a semiconductor liquid junction solar cell*" Iowa State University (1982).
[37] A. Carvalho and A. H. Castro Neto, Phys. Rev. B **89**, 081406 (2014).
[38] A. J. Grant, T. M. Griffiths, G. D. Pitt, A. D. Yoffe, J. Phys. C **8,** L17 (1975).
[39] Y. Du, H. Liu, A. T. Neal, M. Si, and P. D. Ye, IEEE El. Dev. Lett. **34,** 1328 (2013).
[40] L. Yang, K. Majumdar, H. Liu, Y. Du, H. Wu, M. Hatzistergos, P. Y. Hung, R. Tieckelmann, W. Tsai, C. Hobbs, and P. D. Ye, NanoLetters **14,** 6275 (2014).
[41] A. Rai, A. Valsaraj, H. C. P. Movva, A. Roy, R. Ghosh, S. Sonde, S. Kang, J. Chang, T. Trivedi, R. Dey, S. Guchhait, S. Larentis, L. F. Register, E. Tutuc, and S. K. Banerjee, NanoLetters **15,** 4329 (2015).
[42] W. Liu, J. Kang, D. Sarkar, Y. Kahtami, D. Jena, and K. Banerjee, Nano. Lett. **13**, 1983 (2013).